Acta Crystallographica Section D
Biological Crystallography
ISSN 0907-4449

Structures of the γ-class carbonic anhydrase homologue YrdA suggest a possible allosteric switch

Hye-Mi Park,[a]‡ Jeong-Hoh Park,[a,b]‡ Ji-Woo Choi,[a] Jieun Lee,[a] Bo Yeon Kim,[b] Che-Hun Jung[a] and Jeong-Sun Kim[a]*

[a]Department of Chemistry and Institute of Basic Sciences, Chonnam National University, 300 Yongbong-dong, Buk-gu, Gwangju 500-757, Republic of Korea, and [b]Korea Research Institute of Bioscience and Biotechnology, 685-2 Yangcheongri, Cheong-Won, Choongbuk 363-883, Republic of Korea

‡ These authors contributed equally to this work.

Correspondence e-mail: jsunkim@chonnam.ac.kr

Received 24 September 2011
Accepted 18 April 2012

PDB References: YrdA, $P2_1$, 3tio; $P6_3$, 3tis.

The YrdA protein shows high sequence similarity to γ-class carbonic anhydrase (γ-CA) proteins and is classified as part of the γ-CA protein family. However, its function has not been fully elucidated as it lacks several of the conserved residues that are considered to be necessary for γ-CA catalysis. Interestingly, a homologue of γ-CA from *Methanosarcina thermophila* and a β-carboxysomal γ-CA from a β-cyanobacterium have shown that these catalytic residues are not always conserved in γ-CAs. The crystal structure of YrdA from *Escherichia coli* (ecYrdA) is reported here in two crystallographic forms. The overall structure of ecYrdA is also similar to those of the γ-CAs. One loop around the putative catalytic site shows a number of alternative conformations. A His residue (His70) on this loop coordinates with, or is reoriented from, the catalytic Zn^{2+} ion; this is similar to the conformations mediated by an Asp residue on the catalytic loops of β-CA proteins. One Trp residue (Trp171) also adopts two alternative conformations that may be related to the spatial positions of the catalytic loop. Even though significant CA activity could not be detected using purified ecYrdA, these structural features have potential functional implications for γ-CA-related proteins.

1. Introduction

Carbonic anhydrases (CAs) catalyse the interconversion of carbon dioxide and water to bicarbonate and protons in eukarya, archaea and bacteria. Among the five classes of CA, the γ class (γ-CAs) exhibits no significant sequential or structural similarities to the α and β classes (α-CAs and β-CAs; Alber & Ferry, 1994; Hewett-Emmett & Tashian, 1996; Smith *et al.*, 1999).

The γ-CA from *Methanosarcina thermophila* (γ-mtCA; Cam) is iron-dependent *in vivo*, despite capturing zinc ions when overexpressed in *Escherichia coli* (Macauley *et al.*, 2009). It includes a hexapeptide-repeat sequence that is necessary for the formation of a left-handed β-helix fold (Vuorio *et al.*, 1994) and extra amino acids that form one or more α-helices at the C-terminus (Kisker *et al.*, 1996; Peña *et al.*, 2010). It forms a homotrimeric structure mainly through interactions of intervening loops between the β-strands of the left-handed β-helix fold along the central threefold axis (Smith *et al.*, 1999). Three His residues ligating the catalytic metal ion of γ-mtCA (His81, His117 and His122) and three other residues (Glu62, Glu84 and Asn202) are conserved among γ-CAs (Kisker *et al.*, 1996).

Table 1
Data-collection and refinement statistics for ecYrdA.

Values in parentheses are for the highest resolution shell.

Source	BL17A, PF	BL6C, PAL
Wavelength (Å)	1.0000	1.2000
Space group	$P2_1$	$P6_3$
Unit-cell parameters (Å, °)	a = 57.98, b = 84.38, c = 97.76, β = 93.18	$a = b$ = 96.79, c = 87.40, $\alpha = \beta$ = 90, γ = 120
Resolution (Å)	50.0–1.41 (1.43–1.41)	50.0–2.30 (2.38–2.30)
Completeness (%)	99.3 (98.6)	99.2 (98.5)
$R_{\rm merge}$† (%)	3.8 (33.9)	5.9 (26.3)
Reflections (total/unique)	574863/173327	136080/20623
R factor‡/$R_{\rm free}$§ (%)	15.9/19.4	18.0/24.2
No. of atoms		
Protein	8162	4012
Water	956	322
Zinc	6	3
Sulfate	10	0
R.m.s.d.s		
Bonds (Å)	0.004	0.00
Angles (°)	1.36	1.28
Geometry (%)		
Most favoured	98.8	92.9
Generously allowed	1.0	6.1
Disallowed	0.1	1.0

† $R_{\rm merge} = \sum_{hkl}\sum_i |I_i(hkl) - \langle I(hkl)\rangle| / \sum_{hkl}\sum_i I_i(hkl)$, where $\langle I(hkl)\rangle$ is the mean intensity of reflection hkl. ‡ R factor $= \sum_{hkl} ||F_{\rm obs}| - |F_{\rm calc}|| / \sum_{hkl} |F_{\rm obs}|$, where $F_{\rm obs}$ and $F_{\rm calc}$ are the observed and calculated structure-factor amplitudes, respectively, for the reflections hkl included in the refinement. § $R_{\rm free}$ is the same as the R factor but is calculated over a randomly selected fraction (10%) of the reflection data that were not included in the refinement.

Among the mutations of Glu62 in Cam, its replacement by an Asp residue showed CA activity comparable to that of the wild type (Tripp & Ferry, 2000). Mutations of Glu84 induced only small changes in $k_{\rm cat}/K_{\rm m}$. In the bicarbonate complex of a γ-CA homologue from *Pyrococcus horikoshii* (phCaH), for which CA function has not yet been reported, Tyr159 is located at the spatial position of Asn202 in Cam (Jeyakanthan *et al.*, 2008). Substantial CA activity has also been shown for a Cam homologue from *M. thermophila* (CamH) which does not contain the suggested critical Glu84 (Zimmerman *et al.*, 2010). This acidic residue is also replaced by Gln in CcmM (Peña *et al.*, 2010).

Recent bioinformatic analysis of the reported γ-CAs and of related trimeric β-helix structures suggests their subdivision into several functional classes including canonical γ-CAs and putative acetyltransferases/acyltransferases (Fu *et al.*, 2008). The conserved *yrdA* gene in the bacterium encodes a protein of at least ∼180 amino acids and contains hexapeptide-repeat motifs. The sequence may be extended by up to 70 additional amino acids at the N- or C-terminus. The gene product of *yrdA* (YrdA) from *Salmonella enterica* (seYrdA; PDB entry 3r3r; Center for Structural Genomics of Infectious Diseases, unpublished work) shows a similar structure to those of γ-CAs. However, YrdA does not contain residues corresponding to Glu62, Glu84 and Asn202 of the canonical γ-CA (Cam) and could not replace the depleted CA activity of *E. coli* when the β-CA (CynT) was silenced *in vivo* (Merlin *et al.*, 2003).

In this work, we investigate the structure of ecYrdA in two crystal forms in order to obtain further insights into this problematic protein family. Only a small amount of CA activity was observed *in vitro* in the presence of Zn^{2+} and Fe^{2+} ions. Several structural features that have not been reported in related structures are described in detail.

2. Materials and methods

2.1. Cloning, expression and purification of ecYrdA

The *E. coli* gene coding for YrdA (P0A9W9; Met1–Pro184) was amplified from *E. coli* chromosomal DNA by polymerase chain reaction (PCR) using the forward primer 5′-ACGCATATGATGTCTGATGTTTTACGCCATA-3′ and the reverse primer 5′-TACTCGAGAGGCTGGGTCTGGTTACCCTGA-3′. The PCR product was cloned into pET21a (Invitrogen), resulting in a fusion protein with six His residues at the C-terminus. The expression construct was transformed into *E. coli* strain B834 (DE3), which was grown in 1 l LB medium containing ampicillin (100 µg ml^{-1}) at 310 K. After induction by the addition of 1.0 m*M* IPTG, the culture medium was maintained for a further 8 h at 310 K. Cells were harvested by centrifugation at 5000*g* and 277 K. The cell pellet was resuspended in buffer *A* (20 m*M* Tris–HCl pH 7.5, 500 m*M* NaCl) and disrupted by ultrasonication. Cell debris was removed by centrifugation at 11 000*g* for 1 h. The ecYrdA fusion protein was purified using a 5 ml HisTrap chelating column (GE Healthcare, Uppsala, Sweden). The column was extensively washed with buffer *A* and the bound protein was eluted with a linear gradient of 0–500 m*M* imidazole in buffer *A*. After the removal of salts by dialysis against buffer *B* (20 m*M* Tris–HCl pH 7.5), the protein was purified using a 5 ml HiTrap Q anion-exchange column (GE Healthcare, Uppsala, Sweden). The column was extensively washed with buffer *B* and the bound protein was eluted with a linear gradient of 0–1000 m*M* NaCl in buffer *B*. The purified protein was >95% pure according to Coomassie Blue-stained SDS–PAGE. It contained eight extra residues (LEHHHHHH) at the C-terminus.

2.2. Crystallization, data collection and structure determination

For crystallization, the purified ecYrdA was concentrated to 5 mg ml^{-1} in a buffer consisting of 20 m*M* Tris–HCl pH 7.5, 100 m*M* NaCl. Its concentration was determined using an extinction coefficient at 280 nm of 1.132 mg ml^{-1} cm^{-1} calculated from its amino-acid sequence. The initial crystallization conditions for native ecYrdA were obtained by sparse-matrix screening (Jancarik & Kim, 1991). Crystals suitable for diffraction experiments were obtained within 3 d by hanging-drop vapour diffusion at 295 K from precipitant solution 1 [20%(*w*/*v*) polyethylene glycol 4000, 18%(*v*/*v*) 2-propanol, 0.1 *M* sodium citrate pH 5.6] and precipitant solution 2 [20%(*w*/*v*) polyethylene glycol monomethyl ether 2000, 0.15 *M* ammonium sulfate, 0.1 *M* sodium acetate pH 4.6]. For data collection, 10–20%(*w*/*v*) glycerol was added to the respective crystallizing precipitant as a cryoprotectant and the crystals were immediately placed in a 100 K nitrogen-gas stream. Diffraction data were collected from ecYrdA crystals obtained using precipitant solution 1 on the 6C1 beamline of the Pohang Accelerator Laboratory (PAL), Republic of Korea

at a wavelength of 1.2000 Å and were collected from ecYrdA crystals obtained using precipitant solution 2 on the BL17A beamline of the Photon Factory (PF), Japan at a wavelength of 1.0000 Å. The data were indexed, integrated and scaled with the *HKL*-2000 suite (Otwinowski & Minor, 1997). The crystals from precipitant solution 1 were indexed in space group $P6_3$, with unit-cell parameters $a = b = 96.79$, $c = 87.40$ Å, and those from precipitant solution 2 were indexed in space group $P2_1$, with unit-cell parameters $a = 55.98$, $b = 84.38$, $c = 97.76$ Å, $\beta = 93.18^\circ$. The hexagonal $P6_3$ crystal structure of ecYrdA was solved by molecular replacement with *Phaser* v.1.3 (McCoy *et al.*, 2005) using phCaH (PDB entry 1v3w; Jeyakanthan *et al.*, 2008) as a search model. The monoclinic $P2_1$ crystal structure was solved using the refined hexagonal structure as a search model. Further manual model building was performed with *WinCoot* (Emsley & Cowtan, 2004) and *O* (Jones *et al.*, 1991). Refinement was performed with *PHENIX* (Adams *et al.*, 2010) and *CNS* (Brünger *et al.*, 1998). The collected data and refinement are summarized in Table 1.

2.3. Carbonic anhydrase enzymatic assay

The CA activity of ecYrdA was assayed using the Wilbur–Anderson assay method (Wilbur & Anderson, 1948) at several protein concentrations in the presence of Fe^{2+} or Zn^{2+} in a buffer consisting of 20 m*M* Tris–HCl pH 8.3. After blank tests for the pH change from 8.3 to 6.3, the time required for the pH of the sample to decrease from pH 8.3 to 6.3 was measured using each separately purified ecYrdA protein. The Wilbur–Anderson units per millilitre and per milligram were calculated as reported for the Wilbur–Anderson assay. All experiments were performed at 273 K.

3. Results and discussion

3.1. Structural determination and features of ecYrdA

The $P6_3$ crystal structure of ecYrdA was determined by molecular replacement using one protomer of phCaH (PDB entry 1v3w) and was refined to a resolution of 2.3 Å. The monoclinic ecYrdA structure was determined and refined to a resolution of 1.41 Å. phCaH showed ∼35% sequence identity to ecYrdA over ∼170 aligned residues. The asymmetric units of the hexagonal and monoclinic structures contained three and six protein molecules, respectively, with root-mean-square-deviations (r.m.s.d.s) of less than 0.5 Å among the nine superposed protomers. 177 of the 184 residues were modelled in the refined structures, with the exceptions being the first two residues (Met1-Ser2) at the N-terminus and the last five residues (Asn180–Pro184) at the C-terminus. In two of the three protomers of the $P6_3$ system and in one of the six protomers of the $P2_1$ system three to six residues on a loop were partially disordered. The protomer formed 22 β-strands from the N-terminus, with a long α-helix attached at the C-terminus (Glu156–Gly179, αC; Fig. 1).

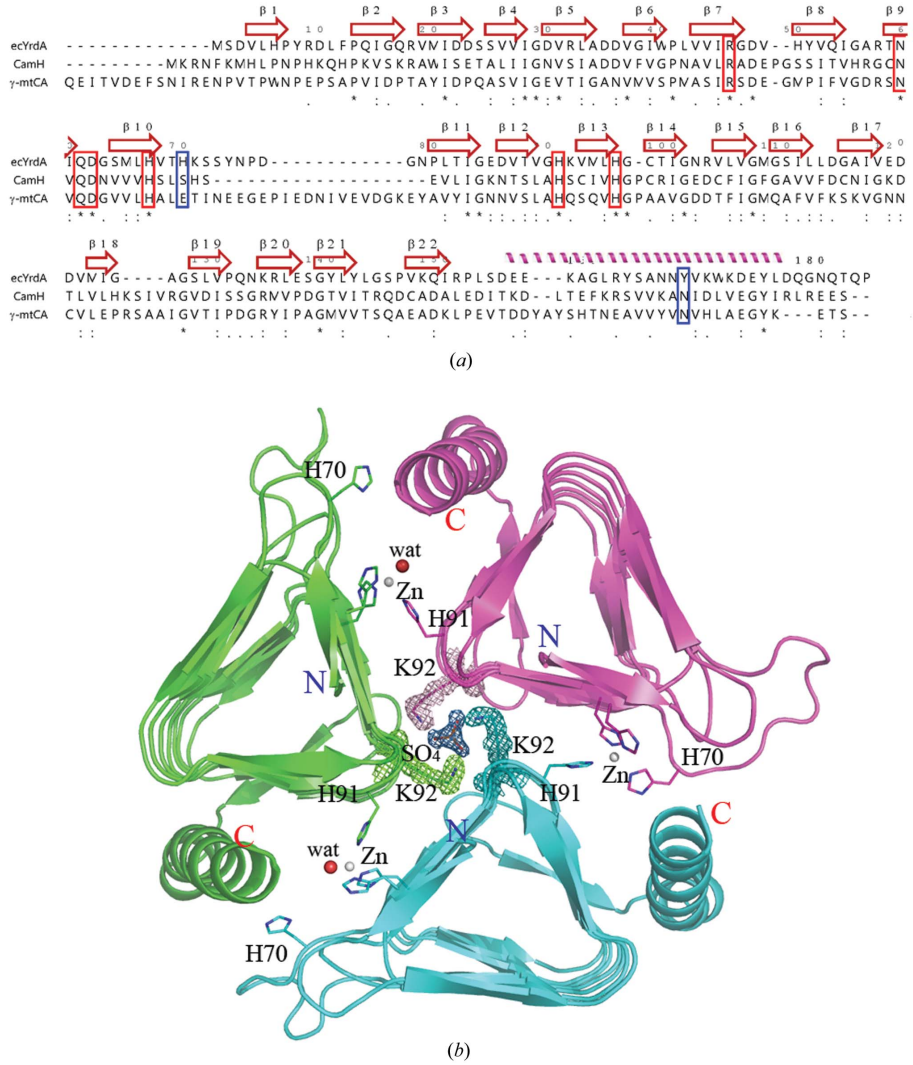

Figure 1
(*a*) Structure-based sequence alignment of YrdA from *E. coli* (ecYrdA), γ-CA from *M. thermophila* (γ-mtCA) and a Cam homologue from *M. thermophila* (CamH). Coils and arrows above the aligned sequences represent α-helices and β-strands, respectively. The numbering follows the amino-acid sequence of ecYrdA. Residues that are identical across all sequences are marked '*'. Conserved residues are marked with ':' or '.'. The conserved residues suggested for catalysis and coordination with the zinc ion are enclosed by red boxes and sequence-variable catalytic residues are shown in blue boxes. (*b*) Ribbon diagram of trimeric ecYrdA complexed with zinc ions at the dimeric interfaces and a sulfate ion at the threefold axis. Each subunit of the trimeric structure is coloured differently (magenta, green and cyan). Zinc ions and water molecules are represented by grey and red balls, respectively. The bound sulfate ion at the threefold axis is shown as a stick model. Except for Fig. 1(*a*), all figures were prepared using *PyMOL* (Schrödinger LLC).

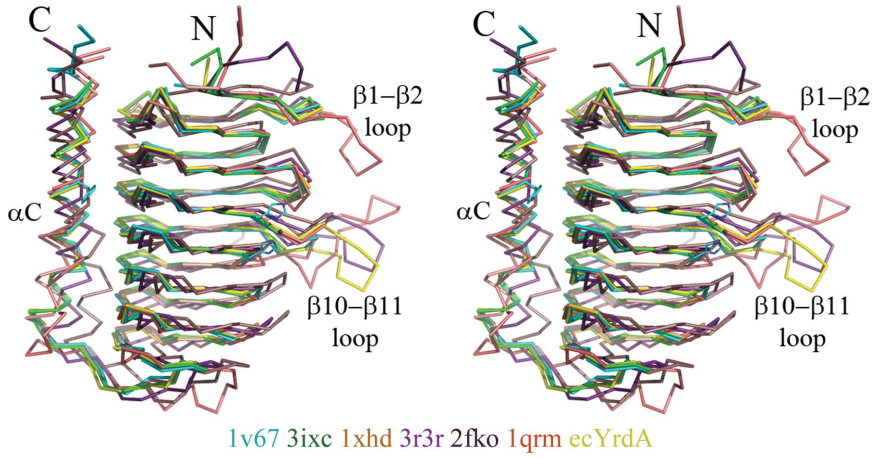

Figure 2
Stereo presentation of monomeric ecYrdA superposed on γ-CAs and related structures. The main-chain atoms of the superposed structures are displayed as ribbon diagrams with different carbon colours and are labelled with their respective PDB codes using similar colours (PDB entry 1qrm corresponds to the structure of Cam and 1v67 to that of phCaH). Sequentially and structurally variable regions around the active sites are indicated.

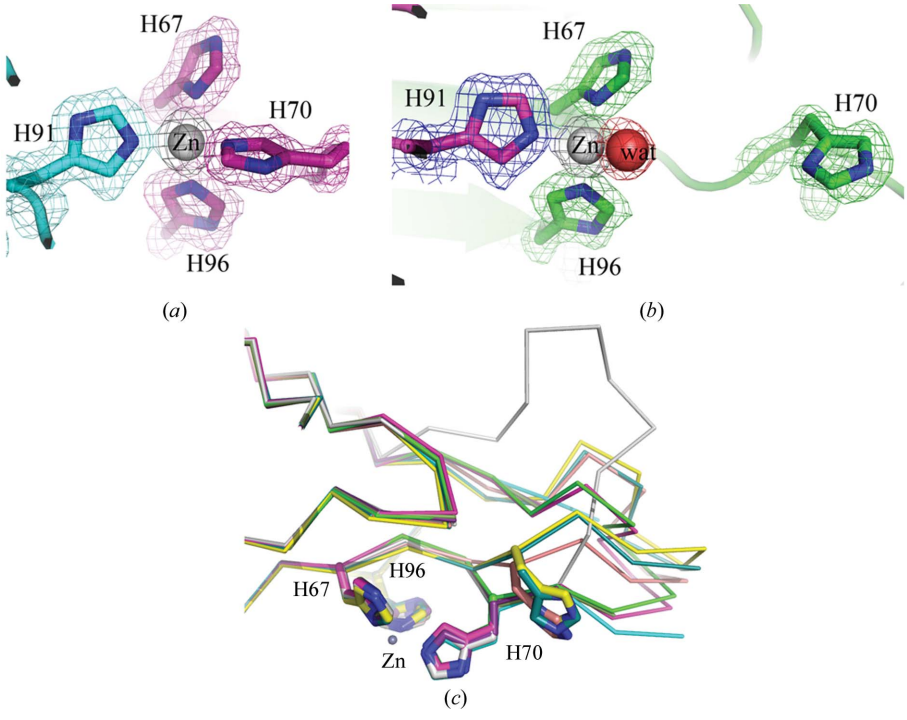

Figure 3
Putative active site and two conformations of the β10–β11 loop. (*a*) Closed conformation. The bound zinc ion (Zn; grey ball) is coordinated by four N atoms of four independent His residues. The subunits are differentiated using cyan and magenta carbon colours. N atoms are represented by blue sticks. The $2F_o - F_c$ electron density for the coordinating His residues and the bound Zn^{2+} at the putative active site are contoured at 1.5σ. (*b*) Open conformation. The bound zinc ion (Zn; grey ball) is coordinated by three His residues originating from two subunits that are differentiated by green and magenta carbon colours. His70 that coordinates to Zn^{2+} in the closed conformation is replaced by a water molecule (wat; red ball). N atoms are represented by blue sticks. The $2F_o - F_c$ density for the coordinating His residues, the bound Zn^{2+} and the water molecule at another putative active site are also contoured at 1.5σ. (*c*) Superposition of putative catalytic sites of ecYrdA. The main-chain atoms of the nine superposed structures are displayed as ribbon diagrams with different colours. The residues coordinating the putative catalytic metal ion (Zn; grey ball) and key residues for metal coordination are represented by stick models.

Analysis of the modelled residues using *PROCHECK* (Laskowski *et al.*, 1993) showed that they were all in valid regions of the Ramachandran plot (Table 1), except for one, Arg9 in the β1–β2 loop region, which showed relatively weak electron density.

DNA-sequencing analysis of the cloned ecYrdA confirmed the presence of a point mutation at a single site (Arg6 to His6) which was introduced during primer synthesis. In the overall structure this replaced residue is exposed to the solvent-accessible region and is not involved in forming the putative active site of ecYrdA or the substrate-binding pocket.

Like other related structures (Fig. 2), the N-terminal β-strands form a triangular prism structure consisting of a left-handed β-helix and interact with the αC helix mostly through hydrophobic interactions on one of its three sides. Several polar interactions were also observed at this interface between the prism structure and the αC helix: the side-chain atom of Lys172 on the αC helix interacts with the peptidyl O atom of Arg18 and Thr88 is hydrogen bonded to Thr164 through their side-chain atoms.

Three trigonal prisms of ecYrdA molecules in the hexagonal system and six in the monoclinic system further assemble to form one and two trimeric structures, respectively. A major contact area for the oligomerization of ecYrdA is provided by the intervening loops between the β-strands of the prisms, which align along the central threefold axes of the trimers. The αC helices of two prisms also aid oligomerization by providing a number of hydrophilic and hydrophobic interactions (Fig. 1*b*). Tyr175 on the αC helix of one subunit is hydrogen bonded to Asp48 on the β7–β8 loop of an adjacent subunit through their side-chain atoms. Gln178 on the αC helix of one protomer interacts with the main-chain N atoms of Arg9 on the β1–β2 loop of a neighbouring protomer. Tyr168 in the αC helix is involved in the oligomerization of the ecYrdA structure and in the formation of a catalytic centre with residues originating from the adjacent molecule.

3.2. Comparison with γ-CAs and other related structures

A search for structural homologues using the *DALI* server (http://www.ebi.ac.uk/dali/) shows that the overall architecture of the trimeric ecYrdA structure is closely related to that of γ-CA proteins (Kisker *et al.*, 1996; Peña *et al.*, 2010), with small r.m.s.d.s of ∼1.5 Å between the superposed molecules. Substantial sequence- and structure-variable regions are observed at each terminus, with added extra amino acids (Figs. 1*a* and 2).

Another sequence-variable region is present in the middle of the aligned sequences (Fig. 1*a*); it forms a loop between the β10 and β11 strands (the β10–β11 loop; an acidic loop) and includes an acidic residue (Glu84) near the catalytic site of canonical γ-CAs (Figs. 2 and 3). Although this region possesses the common structural feature of a loop, there are intrinsic differences from the related proteins (Fig. 1*a*). While fewer than four amino acids form short turns in phCaH (Jeyakanthan *et al.*, 2008) and YrdAs (PDB entries 1xhd and 2eg0), the β1–β11 loops in the other proteins are composed of ∼10 amino acids (Kisker *et al.*, 1996; Peña *et al.*, 2010). Structural diversity of these loops was observed within the trimers of the refined ecYrdA structures. Three different spatial positions for the β10–β11 loop were found in the nine molecules of the two crystal forms: the electron density of three protomers in one conformation was too weak to allow these residues to be traced, while the remaining six molecules had a defined electron density regardless of the conformation (Fig. 3*c*).

The β1–β2 loop also shows an interesting difference in the construction of a pocket around the active site; its structural features are described later. Structural deviations were also observed in the αC helix and the β22–αC loop (Fig. 2), with the latter also showing sequence diversity.

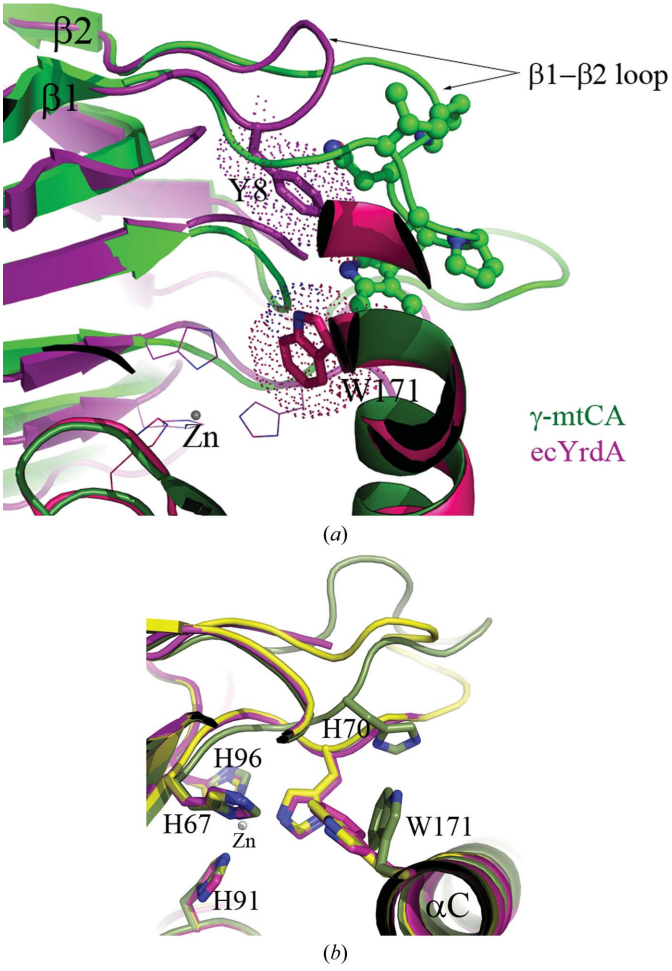

Figure 4
Comparison of active sites. (*a*) Differences in the β1–β2 loops between superposed ecYrdA and γ-mtCA. The main-chain atoms of the two superposed structures are displayed as differently coloured ribbon diagrams (green for γ-mtCA and magenta for ecYrdA). The residues involved in coordinating a metal ion (Zn; grey ball) and some residues involved in forming the pocket of the active site are represented by ball-and-stick models for γ-mtCA and by stick models for ecYrdA. The surfaces of Tyr8 and Trp171 are shown as dots. (*b*) Two alternative conformations of Trp171 around the active site of ecYrdA. The superposed catalytic sites of trimeric ecYrdA including the β10–β11 loop regions observed in the present structures are displayed as ribbon diagrams with different carbon colours. Residues coordinating the Zn^{2+} ion (Zn; grey ball) and Trp171 with rotameric conformations are represented by stick models.

3.3. Putative active site of ecYrdA

γ-CAs and related proteins are likely to show diverse functionality depending on the conservation of catalytic residues. Nonetheless, they all require metals, with Zn^{2+} or Fe^{2+} ions coordinating at the interfaces with three protein atoms from the two close protomers and one or two water molecules (Kisker *et al.*, 1996). The product of γ-CA, bicarbonate, has been found close to this bound zinc ion (Iverson *et al.*, 2000; Peña *et al.*, 2010), indicating that catalysis occurs at these interfaces.

Despite the fact that no metal ions were added during the purification and crystallization of ecYrdA, strong electron densities were observed at the nine interfaces of both crystal forms (Figs. 1*b* and 3). This electron density is coordinated by four ligands: either four His residues or three His residues and a water molecule. X-ray absorption fine-structure (XAFs) spectroscopy performed on various metal ions using a synchrotron-radiation source suggested the presence of Zn ions in the crystals (data not shown). The anomalous difference map identified these strong electron densities as Zn^{2+} ions that were likely to have been taken up from the medium during the expression and purification of ecYrdA. The locations of the Zn^{2+} ions in ecYrdA coincide with those in Cam and structurally related proteins. These structural features strongly suggest that the region around the zinc ion-binding site may be the catalytic site of ecYrdA.

The β1–β2 loop (Figs. 2 and 4*a*) is another feature; it contributes to the formation of the active sites of ecYrdA, γ-mtCA and CcmM (Kisker *et al.*, 1996; Peña *et al.*, 2010). This loop comprises eight amino acids in γ-mtCA (Fig. 1*a*), including the bulky Trp19, and contributes to the formation of the active pocket of γ-mtCA (Figs. 2 and 4*a*). In ecYrdA this loop includes only three amino acids (Fig. 1*a*) and forms a short turn which hosts the bulky residues Tyr8 in the β1 strand

of one protomer and Trp171 in the αC helix on the adjacent protomer (Fig. 4*a*), resulting in a space around the active site of ecYrdA that is similar to that of γ-mtCA. Trp171 in ecYrdA, corresponding to Leu205 in γ-mtCA, shows two rotameric conformations (Fig. 4*b*). When it is located away from the active site, the β10–β11 loop is also distant from the active site or not properly traced. When Trp171 is close to the active site all of the residues in the β10–β11 loop are correctly positioned, implying that the relative orientation of the β10–β11 loop is at least partially dependent upon Trp171.

Based on this structural background and the absence of conserved residues critical to catalysis in CamH, the CA activity of ecYrdA was assessed in the presence of Zn^{2+} and Fe^{2+} ions using the Wilbur–Anderson assay (Wilbur & Anderson, 1948). However, ecYrdA showed an activity of less than ∼8 Wilbur–Anderson units per milligram (WAU; data not shown) in all measured cases, which is fairly small compared with other reported CAs (several hundred WAU; Mitra *et al.*, 2004). The absence of significant CA activity in ecYrdA also suggests that the equivalent of Glu62 and/or Asn202 of γ-mtCA may be required for CA activity.

3.4. Conformation of the β10–β11 loop

Small differences were observed around the active site of ecYrdA in comparison with other similar structures (Fig. 3). γ-CAs and their related proteins commonly include metal ions intermolecularly coordinated by three His residues and one or two water molecules (Kisker *et al.*, 1996; Peña *et al.*, 2010), which is denoted the open conformation.

An alternative closed conformation was observed in both ecYrdA crystal structures (Fig. 3). In four of the six molecules of the $P2_1$ system and in two of the three molecules of the $P6_3$ system, His70 in the acidic β10–β11 loop coordinates the Zn^{2+} ion together with N atoms from His67 and His96 in one protomer and His91 in the adjacent protomer (Figs. 1*b* and 3*a*), which is denoted the closed conformation. In the other three protomers of the two crystal systems open conformations are formed (Figs. 1*b* and 3*b*). In the monoclinic $P2_1$ system all three protomers of one trimeric structure maintain closed conformations; the other trimeric structure has two protomers in an open conformation and one in a closed conformation. The trimer in the hexagonal system includes one protomer in an open conformation and two in closed conformations. However, only open conformations are observed in related structures, including γ-CAs and seYrdA, which contain ∼10 residues in the β10–β11 loop (Iverson *et al.*, 2000; Jeyakanthan *et al.*, 2008; Kisker *et al.*, 1996; Peña *et al.*, 2010). We checked whether the conformational change observed in ecYrdA was derived from the intermolecular contacts, but we could not derive a common relationship between the crystal packing and the conformational changes. During the conformational change of ecYrdA from the open to the closed state (Fig. 3*c*), 11 amino acids in the acidic loop His70–Pro80 show alternative conformations. Among them, the four amino acids (Tyr74–Asp77) in the middle of the loop exhibit the largest spatial displacement at ∼9.5 Å, with a maximum of 10.1 Å between the CA atoms of Tyr74. The residues His70 and Pro80 display the smallest spatial movements of 1.44 and 2.57 Å, respectively. Interestingly, the side chain of His70, which has a small spatial movement, is likely to be profoundly affected by the main-chain movement of the loop, resulting in the coordination or release of Zn ions in both conformations.

Three metal-coordinating His residues (His67, His91 and His96) are stabilized by nearby residues in both conformations. The side chains of His96 and Asp114 interact with each other and His91 forms hydrogen bonds to Asp62. The orientation of His67 is also fixed through interactions with the side-chain atoms of Asp48. However, no residues are observed to restrict the side chain of His70 in either conformation, which may be the cause of its possible alternative orientations in the ecYrdA structure and further reflects the flexibility of the β10–β11 loop. As indicated above, the rotameric conformation of Trp171 appears to be partially related to the orientation of His70.

4. Concluding remarks

The crystal structures of ecYrdA indicate that YrdA belongs to the γ-CA family at the structural level as well as at the sequence level. The acidic loop near the Zn^{2+} ion shows several conformations, resulting in ligation of the Zn^{2+} ion by His70 or one water molecule (Fig. 3), which may imply two aspects of ecYrdA function. Firstly, Asp44 in the tense state replaces the catalytic water molecule in the relaxed state of β-CA from *Haemophilus influenza* (β-hiCA). Despite the lack of sequence conservation between Asp44 in β-hiCA and His70 in ecYrdA, the replacement of a catalytic water molecule in ecYrdA and its switching between two conformations (Fig. 3) are similar to the relaxed and tense states of β-hiCA (Cronk *et al.*, 2006; Rowlett *et al.*, 2009). However, significant CA activity was not detected for purified ecYrdA (data not shown), making it uncertain whether this feature is relevant to understanding the better studied γ-CAs.

Secondly, the loop around the active site is closely related to the formation of a substrate-binding pocket. The highly flexible acidic loop here may alternatively suggest that ecYrdA prefers a larger substrate than the carbonate substrate of γ-CA proteins. However, this is remains unclear since the function of ecYrdA has not yet been characterized. Therefore, further work is required to reach any definitive conclusion that would explain the structural features obtained here.

This work was supported by the World Class Institute (WCI) Program of the National Research Foundation of Korea (NRF) funded by the Ministry of Education, Science and Technology of Korea (MEST; NRF grant No. WCI 2009-002) and by the Basic Science Research Program through the National Research Foundation of Korea funded by the Ministry of Education, Science and Technology (2010-0008560 and 2011-0003900). The authors wish to thank the staff

scientists at PAL and PF for their assistance with data collection.

References

Adams, P. D. *et al.* (2010). *Acta Cryst.* D**66**, 213–221.

Alber, B. E. & Ferry, J. G. (1994). *Proc. Natl Acad. Sci. USA*, **91**, 6909–6913.

Brünger, A. T., Adams, P. D., Clore, G. M., DeLano, W. L., Gros, P., Grosse-Kunstleve, R. W., Jiang, J.-S., Kuszewski, J., Nilges, M., Pannu, N. S., Read, R. J., Rice, L. M., Simonson, T. & Warren, G. L. (1998). *Acta Cryst.* D**54**, 905–921.

Cronk, J. D., Rowlett, R. S., Zhang, K. Y. J., Tu, C., Endrizzi, J. A., Lee, J., Gareiss, P. C. & Preiss, J. R. (2006). *Biochemistry*, **45**, 4351–4361.

Emsley, P. & Cowtan, K. (2004). *Acta Cryst.* D**60**, 2126–2132.

Fu, X., Yu, L.-J., Mao-Teng, L., Wei, L., Wu, C. & Yun-Feng, M. (2008). *Mol. Phylogenet. Evol.* **47**, 211–220.

Hewett-Emmett, D. & Tashian, R. E. (1996). *Mol. Phylogenet. Evol.* **5**, 50–77.

Iverson, T. M., Alber, B. E., Kisker, C., Ferry, J. G. & Rees, D. C. (2000). *Biochemistry*, **39**, 9222–9231.

Jancarik, J. & Kim, S.-H. (1991). *J. Appl. Cryst.* **24**, 409–411.

Jeyakanthan, J., Rangarajan, S., Mridula, P., Kanaujia, S. P., Shiro, Y., Kuramitsu, S., Yokoyama, S. & Sekar, K. (2008). *Acta Cryst.* D**64**, 1012–1019.

Jones, T. A., Zou, J.-Y., Cowan, S. W. & Kjeldgaard, M. (1991). *Acta Cryst.* A**47**, 110–119.

Kisker, C., Schindelin, H., Alber, B. E., Ferry, J. G. & Rees, D. C. (1996). *EMBO J.* **15**, 2323–2330.

Laskowski, R. A., MacArthur, M. W., Moss, D. S. & Thornton, J. M. (1993). *J. Appl. Cryst.* **26**, 283–291.

Macauley, S. R., Zimmerman, S. A., Apolinario, E. E., Evilia, C., Hou, Y.-M., Ferry, J. G. & Sowers, K. R. (2009). *Biochemistry*, **48**, 817–819.

McCoy, A. J., Grosse-Kunstleve, R. W., Storoni, L. C. & Read, R. J. (2005). *Acta Cryst.* D**61**, 458–464.

Merlin, C., Masters, M., McAteer, S. & Coulson, C. (2003). *J. Bacteriol.* **185**, 6415–6424.

Mitra, M., Lato, S. M., Ynalvez, R. A., Xiao, Y. & Moroney, J. V. (2004). *Plant Physiol.* **135**, 173–182.

Otwinowski, Z. & Minor, W. (1997). *Methods Enzymol.* **276**, 307–326.

Peña, K. L., Castel, S. E., de Araujo, C., Espie, G. S. & Kimber, M. S. (2010). *Proc. Natl Acad. Sci. USA*, **107**, 2455–2460.

Rowlett, R. S., Tu, C., Lee, J., Herman, A. G., Chapnick, D. A., Shah, S. H. & Gareiss, P. C. (2009). *Biochemistry*, **48**, 6146–6156.

Smith, K. S., Jakubzick, C., Whittam, T. S. & Ferry, J. G. (1999). *Proc. Natl Acad. Sci. USA*, **96**, 15184–15189.

Tripp, B. C. & Ferry, J. G. (2000). *Biochemistry*, **39**, 9232–9240.

Vuorio, R., Härkönen, T., Tolvanen, M. & Vaara, M. (1994). *FEBS Lett.* **337**, 289–292.

Wilbur, K. M. & Anderson, N. G. (1948). *J. Biol. Chem.* **176**, 147–154.

Zimmerman, S. A., Tomb, J. F. & Ferry, J. G. (2010). *J. Bacteriol.* **192**, 1353–1360.